ANTIOXIDANTS & REDOC SIGNALING
Volume 9, Number 7, 2007

DOI: 10.1089/ars.2007.1551

Original Research Communication

Nitric Oxide Regulation of Microvascular Oxygen

DONALD G. BUERK

ABSTRACT

The role of nitric oxide (NO) as a highly diffusible free radical gaseous vasodilator is intrinsically linked to the control of blood flow and oxygen (O_2) delivery to tissue. NO also is involved in regulating mitochondrial O_2 metabolism, growth of new blood vessels, and blood oxygenation through control of respiratory ventilation. Hemoglobin and myoglobin may help to conserve NO for subsequent release of a NO-related vasoactive species under hypoxic conditions. NO has a major role in regulating microvascular O_2, and dysfunctional NO signaling is associated with the pathogenesis of metabolic and cardiovascular diseases. *Antioxid. Redox Signal.* 9, 829–843.

INTRODUCTION

In the past two decades since NO was identified as the endothelium-derived relaxing factor (50, 101), it is now accepted that NO plays a key role in the regulation of vascular tone (for a historical review, see Ref. 87). Another recognized major role for NO is inhibition of platelet adhesion and aggregation, to help maintain unimpeded blood flow through the microcirculation. Many other biological functions for NO and related chemical species have been established. New roles for NO continue to emerge as the surprisingly complex and rich biochemistry of this simple gaseous molecule with free radical properties is revealed.

NITRIC OXIDE SYNTHASES AND OTHER SOURCES OF NO

NO production by nitric oxide synthase (NOS) enzymes requires the conditionally essential amino acid L-arginine, O_2, and other necessary cofactors (88, 100). Three major NOS isoforms have been identified in many different organs and tissues: the constitutive intracellular Ca^{2+}/calmodulin-dependent neuronal (nNOS) and endothelial (eNOS) isoforms, and the inducible (iNOS) Ca^{2+}/calmodulin-independent isoform (119). It has been possible to investigate the functional importance of NOS with the development of knockout mouse models for individual NOS isoforms (47, 48, 139), double knockout mice (114), and recently, triple knockout mice (132). There is a growing body of evidence for a fourth isoform (mtNOS) located in mitochondria (see ref. 40 for review), although there is also evidence that does not support the existence of mtNOS (31, 64).

In addition to enzymatic sources of NO, there appear to be substantial storage pools from which NO can be released independently from NOS activity (149). Nitrite (NO_2^-) may be the most significant storage pool. NO_2^- can be converted to NO under ischemic or hypoxic conditions (16). Red blood cells (RBCs) are important regulators of NO_2^- transport (30, 41). NO or related reactive species can modify proteins, forming *S*-nitrosothiols, *S*-nitrosoalbumin, and other *S*-nitrosoprotein species under normal physiological conditions (45). NO may react directly with thiols in an O_2-dependent manner (44). Other reaction pathways for NO modified thiols and lipids have been reviewed (104). Hemoglobin (Hb) may also serve as a storage pool for NO through formation of *S*-nitrosohemoglobin (SNO-Hb) (116), although there is still some controversy on what biochemical reactions between NO and Hb are the most physiologically relevant (55). A similar NO storage mechanism has been proposed as NO reacts with myoglobin (Mb) to form *S*-nitrosomyoglobin (SNO-Mb) (105). Neuroglobin, a myoglobin-like hemeprotein in the

Departments of Physiology and Bioengineering, University of Pennsylvania, Philadelphia, Pennsylvania.

brain and possibly other tissues may also scavenge NO, and might also act as a sensor for the O_2/NO ratio (15).

FACTORS THAT DETERMINE NOS ACTIVITY

A simplified schematic outline for the production of NO by NOS and many of the other associated biochemical pathways is shown in Fig. 1. Two molecules of O_2 are required for the two-step oxidation of L-arginine (120). The intermediate oxidation product, N^G-hydroxy-L-arginine (NOHA), can inhibit arginase activity (21), which is competing for L-arginine substrate. The Michaelis–Menten constant (K_m) for O_2 varies with different NOS isoforms, as reviewed by Buerk (17). The O_2 partial pressure (PO_2) in the bloodstream near endothelial cells is usually well above the K_m for O_2 used by eNOS (K_m < 10 Torr) so O_2 availability is unlikely to be a limiting factor for NO production by eNOS under normal conditions in the microcirculation, even in venules. However, this may not be the case for nNOS or iNOS, which appear to have much higher K_m values for O_2 (see Ref. 7), and are usually located at some distance from the bloodstream. The K_m for O_2 has been reported to vary between 11–22 Torr for kidney, liver, and brain mtNOS, and was found to be highest for brain mtNOS (1).

In addition to NO, NOS also produces L-citrulline, which is converted back to L-arginine through argininosuccinate lysate activity in the kidneys (34). Dietary sources for L-arginine include conversion of L-glutamine and L-glutamate to L-citrulline in the small intestine. L-Arginine is also synthesized in the liver (138), but is mainly catabolized in the urea cycle through arginase (type 1) activity (102). Intracellular L-arginine is reported to range between 0.1–2 m*M* (4, 10, 81), which is far in excess of eNOS enzymatic requirements. The K_m for L-arginine of the different NOS isoforms is reported to range between 1–32 μ*M*, and is highest for iNOS (10, 106, 130). Even with this high bioavailability of L-arginine, some *in vitro* studies (75, 122) report that excess L-arginine causes an increase in NO production. This unexpected effect is known as the "L-arginine paradox" (62), although the mechanisms for this response are not clear. One possibility is that NOS activity is linked to the rate of L-arginine transport and not to intracellular concentration. There is evidence (81, 109) for co-localization of eNOS and the L-arginine cationic amino acid transporter (CAAT) in caveolae (63), which may limit L-arginine bioavailability.

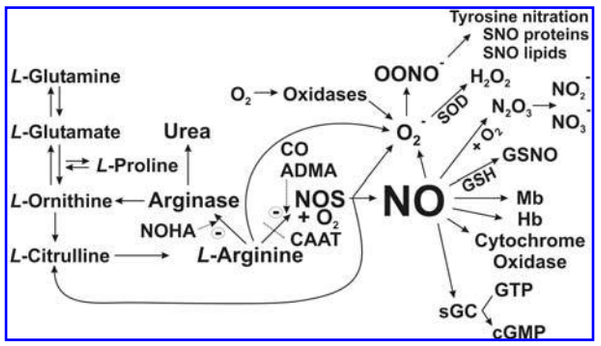

FIG. 1. Schematic outline for O_2-dependent enzymatic production of NO from L-arginine by NOS, competition for L-arginine, and other downstream reactions for NO (see text for additional description of pathways).

In addition to O_2 and L-arginine, tetrahydropterin (BH_4) and nicotinamide–adenine–dinucleotide phosphate (NADPH) are necessary cofactors for NO production by NOS. BH_4 is synthesized by guanidine triphosphate cyclohydrolase (GTPCH) and associated intermediate reaction pathways, which require magnesium, zinc, and NADPH. Oxidized forms of BH_4 are salvaged via sepiapterin and sepiapterin reductase, by dihydrofolate reductase *via* folic acid (folate) metabolism, and by dihydropterine reductase (see Ref. 86 for review). Reduced bioavailability of BH_4 may occur by decreased expression of GTPCH due to oxidative stress (143), or by oxidation of BH_4 to BH_2. An increase in peroxynitrite ($ONOO^-$) generated from the extremely rapid reaction between NO and superoxide (O_2^-) in competition with elimination of O_2^- *via* SOD (17) can be one mechanism for oxidizing BH_4 (83).

Chen and Popel (26) mathematically modeled NO production by eNOS, using kinetic rate parameters estimated from the literature for *in vitro* studies with cultured endothelial cells and other biochemical studies. A coupled set of 15 differential equations for the major chemical species was solved. O_2-dependent NOS activity and the kinetics for NAPDH use were not included in the model. The model predicted that the steady-state NO production rate (R_{NO}) for endothelial cells should range between 0.01 to 0.095 μ*M* s^{-1}. However, the authors pointed out that this prediction falls below most experimental R_{NO} values from *in vitro* studies, by as much as two orders of magnitude. R_{NO} values in the 10–12 μ*M* s^{-1} range, depending on shear stress, have been estimated from measurements of total nitrite (NO_2^-) and nitrate (NO_3^-) generated by cultured endothelial cells (61, 78). Higher values for R_{NO}, ~70 μ*M* s^{-1}, have been used in some mathematical models for NO transport, based on an analysis (136) of *in vitro* experimental NO microelectrode measurements from aortic vessel segments (79).

UNCOUPLED NOS AND ENDOTHELIAL DYSFUNCTION

"Endothelial dysfunction" is generally identified with either reduced biological availability of NO or less effective vasodilation by NO. This may also be associated with an imbalance in release of other vasoactive substances generated by the endothelium. It is significant that triple knockout mice lacking eNOS, nNOS, and iNOS genes have lower survival rates compared with wild-type mice or mice with single or double NOS gene deletions. These mice manifested multiple symptoms of cardiovascular and metabolic disease, including hypertension, hypertriglyceridemia, impaired glucose tolerance, severe insulin resistance, visceral obesity, myocardial infarction associated with severe atherosclerotic lesions, and nephrogenic diabetes insipidus with renal damage (132).

Reactive O_2 species (ROS), reactive nitrogen species (RNS), and impaired antioxidant defenses are associated with metabolic and cardiovascular diseases. Sources of ROS/RNS

include the mitochondrial electron transport chain, lipoxygenase, cyclooxygenase, cytochrome P_{450} enzymes, NADPH oxidase, and xanthine oxidase (see Refs. 73, 96, 133 for reviews). A computer simulation for the chemistry of RNS by Lancaster (70) suggests that, under physiologically relevant conditions in the presence of carbon dioxide (CO_2), nitrosation and nitration are relatively minor reactions, and that mostly oxidative reactions are predicted to occur, primarily through the oxidizing species carbonate ion (CO_3^-), nitrogen dioxide (NO_2), and $ONOO^-$. Deficiencies in L-arginine or BH_4 availability have been linked to increased generation of O_2^- by NOS (uncoupled NOS) with increased incidence of cardiovascular diseases (see Refs. 49, 86, 92 for reviews). Asymmetric dimethylarginine (ADMA), an analogue of L-arginine, may directly inhibit eNOS (10, 130). Elevated ADMA levels in blood plasma are thought to be a risk factor in hypercholesterolemia, diabetes mellitus, hypertension, chronic heart failure, coronary artery disease, erectile dysfunction, and other cardiovascular diseases (9, 85, 148).

L-Arginine is also required for other metabolic pathways (89) which could compete for L-arginine and potentially limit its availability for NO production by NOS. A major pathway is the hydrolization of L-arginine into urea and L-ornithine by the enzyme arginase (*left side* of Fig. 1). Steppan *et al.* (117) have found that arginase II in rat heart is confined to mitochondria and competes for L-arginine used by nNOS, which produces NO to modulate cardiac contractility through ryanodine receptors. There is ample evidence that upregulation of arginase contributes to the pathophysiology of vascular disease processes including aging (117), erectile dysfunction associated with diabetes (8), hypertension (32, 51), atherosclerosis (84), and reactive airways disease associated with asthma (82, 145).

There has been interest in using dietary supplementation of L-arginine to improve cardiovascular health, and there is some evidence for reversal of endothelial dysfunction associated with cardiovascular disease (Lerman *et al.* 1998, Blum *et al*. 1999, Maxwell *et al.* 2000). Lass *et al.* (74) report that L-arginine is a scavenger of O_2^-. Therefore, excess L-arginine might limit the amount of $ONOO^-$ formed. However, the major portion of excess L-arginine from dietary supplements may be metabolized in the liver, entering the urea cycle *via* arginase activity (*left side* of Fig. 1) and not be available to NOS enzymes. There is also interest in supplementing BH_4, and clinicial trials are currently underway for a stable compound that may have potential therapeutic benefit.

SOLUBLE GUANYLATE CYCLASE AND OTHER NO TARGETS

Major NO targets and NO reaction pathways are indicated at the *bottom right side* of Fig. 1. The catalytic heme site in soluble guanylate cyclase (sGC) is generally recognized to be the primary target for NO, activating the conversion of guanosine triphosphate (GTP) to 3',5′-cyclic guanosine monophosphate (cGMP) (33), causing relaxation of vascular smooth muscle. It was initially thought that sGC activation was a simple "on–off" mechanism with a protein conformation change that occurred when NO was bound to the heme site. It was not clear how NO could compete for O_2, which would be present at much higher concentrations than NO, or why sGC was deactivated much slower *in vitro* than *in vivo*. Boon *et al.* (12) propose that the absence of a distal pocket tyrosine near the heme site eliminates O_2 binding. It now appears that sGC is able to regulate two types of cGMP signals; a tonic response to basal NO levels that is long lasting and produces low levels of cGMP, and an acute response that can generate a shorter lasting, large increase in cGMP synthesis (see Ref. 25 for review). However, it is not clear what the different NO levels are for the two types of sGC activation.

A more continuous change in activation of sGC by NO is predicted from a model for the NO/cGMP pathway in vascular smooth muscle cells by Yang *et al.* (140). The model is based on NO binding at two catalytic sites, using a negative feedback loop with cGMP concentration as a control mechanism to inhibit sGC activity. This approach results in a Michaelis–Menten type of relationship between NO and cGMP that can be shifted towards increased sensitivity at lower NO concentrations, depending on the amount of negative feedback gain. They also simulated how intracellular Ca^{2+} would vary as NO changes sCG activity, based on cGMP activation of large conductance potassium/calcium ion channels, which in turn allowed predictions for how the relative force generated by smooth muscle would vary as a function of intracellular Ca^{2+}. The authors note that there are many other mechanisms that were not included in the model which might also have an impact on sGC activation by NO. As reviewed by Cary *et al.* (25), adenosine 5′-triphosphate (ATP), nucleotides and purine-like molecules also affect the sGC catalytic site. ATP inhibits sCG activity (107, 121), which provides another link between NO and microvascular O_2 through mitochondrial ATP production. An additional link is that RBCs release ATP in response to decreased O_2, more acidic pH, and mechanical deformation (7, 37, 115), and that NO inhibits ATP release from RBCs (94, 95).

REVERSIBLE INHIBITION OF MITOCHONDRIAL RESPIRATION BY NO

As reviewed by Buerk (17), it has been known for some time that NO competes with O_2 and reversibly inhibits mitochondrial O_2 consumption by the terminal respiratory chain enzyme cytochrome *c* oxidase (14, 29). In that review, a linear relationship for the increase in apparent K_m for O_2 consumption with NO was proposed, based on experimental results in the literature (14, 59). This relationship predicts that the apparent K_m will double at a NO concentration = 27 n*M* compared to the K_m for O_2 consumption in the absence of NO. Antunes *et al.* (3) developed a single catalytic site model for inhibition of O_2 consumption based on purely competitive molecular mechanisms at the heme O_2 binding site, which predicts that inhibition of mitochondrial O_2 consumption is greater when the O_2/NO ratio is high, with a lesser effect when tissue PO_2 is low. The single-site model also predicts that NO is a weaker inhibitor when O_2 consumption and enzyme turnover is low. Mason *et al.* (80) propose a two-site mechanism, where an adjacent copper site can bind NO at lower affinity with noncompetitive kinetics. NO binding was

compared with carbon monoxide (CO) binding using either purified cytochrome c oxidase or submitochondrial particles, with simultaneous NO and O_2 electrode measurements in a reaction chamber in the absence of light to avoid photosensitive effects on CO or NO binding. It has been known for many years that CO also inhibits O_2 consumption (103). However, NO is a much more effective inhibitor, by a factor of 1,000 to 2,000 in the study by Mason *et al.* (80). They reported that NO inhibition of cytochrome c oxidase activity was strongly dependent on enzyme turnover, which is also consistent with the single site competitive model by Antunes *et al.* (3). However, only the two-site model was able to describe the full range of data obtained in the study by Mason *et al.* (80). At low turnover rates, they found that cytochrome c oxidase activity was half-maximal when NO = 84 n*M*, but at high turnover rates, half-maximal activity occurred when NO = 1170 n*M*. The two-site model predicts that NO can be a more effective inhibitor than predicted by the single-site model, especially when O_2 consumption is low. Palacios–Callender *et al.* (97) note that cytochrome c oxidase does not operate at full capacity, and show that the addition of electron donors to iNOS-transfected cells results in inhibition of respiration by NO at progressively higher O_2 levels. They propose that cytochrome c oxidase is able to compensate by increasing electron transfer to maintain respiration, up to a finite maximum rate, as NO increases. Cells with a high demand for ATP require a higher electron transfer rate, and would have less capacity to maintain respiration as NO increases.

There have been relatively few attempts to incorporate inhibition of O_2 consumption by NO into mathematical models for O_2 transport. The first model to include inhibition of O_2 consumption by NO was described for vessels in planar geometry by Thomas *et al.* (128), based on experimental estimates for NO scavenging rates in tissue. We include the reversible inhibition of O_2 metabolism in our mathematical models for coupled NO and O_2 transport in cylindrical geometry that is more representative of small arterioles, for a wide range of conditions (19, 27, 28, 67–69). In general, these models demonstrate that when the source of NO is primarily from the endothelium, O_2 consumption is inhibited to a greater extent in the region of tissue nearest the endothelium where NO levels are higher, compared with distances further away as NO is scavenged in the surrounding tissue and disappears. However, inhibition of O_2 consumption in the well-oxygenated region closest to the arteriole allows more O_2 to diffuse deeper into the surrounding tissue, preventing hypoxic conditions. This effect is even greater in models which include additional NO production by nNOS, iNOS, or mtNOS in the surrounding tissue (19, 68). The relatively simple relationship that we used to represent the effect of NO on O_2 consumption in these models will need to be revised to reflect more complex mechanisms for the interaction between NO and cytochrome c oxidase (80, 97).

The inhibition of O_2 consumption by NO is the most probable explanation for the differences in intravascular and extravascular PO_2 measured by O_2 phosphorescence quenching methods in the microcirculation of wild-type and eNOS-knockout mice by Cabrales *et al*. (23). From optical measurements through dorsal chamber windows in conscious mice, they found that PO_2 was significantly lower in arterioles, tissue, and venules in the eNOS-knockout mice compared with wild-type mice, despite the fact that there was no statistically significant difference in microvascular parameters such as vessel diameter, blood velocity, volumetric flow rate, and functional capillary density. There were some significant differences between the mice. The eNOS-knockout mice had a higher mean arterial blood pressure and fewer arterioles in the window preparation than the wild-type mice. The calculated longitudinal loss of O_2 down the length of arterioles was ~40% higher in the eNOS knockout mice compared with wild-type mice. Cabrales *et al.* (23) concluded that eNOS knockout mice had greater tissue O_2 consumption than wild-type mice, presumably due to the lack of NO inhibition of O_2 consumption in the tissue surrounding the microvasculature. However, they noted that the transmural PO_2 gradients measured from the centerline of blood flow in the vessel to immediately outside the vessel wall were actually smaller for the eNOS-knockout mice. This suggests that vascular wall O_2 consumption did not increase as expected with the lack of eNOS-derived NO to inhibit O_2 consumption, but instead was lower compared with wild-type mice. However, the longitudinal PO_2 gradient was significantly greater for the eNOS-knockout mice. The effects of NO on inhibiting tissue O_2 consumption in the wild-type mice probably accounts for the differences in their microvascular PO_2 observations.

Shibata *et al.* (110–112) have conducted similar O_2 phosphorescence quenching studies of the microcirculation in the rat cremaster muscle, and measured transmural O_2 gradients as a method to evaluate changes in vascular wall O_2 consumption under different conditions, including nonselective inhibition of NOS activity with N^{ω}-nitro-L-arginine methyl ester (L-NAME). They concluded that there was an increase in vascular wall O_2 consumption after inhibiting NOS (111, 112). However, they attributed this finding to an increase in the workload for smooth muscle in the constricted vascular wall, and not to the loss of the inhibitory effect of NO on O_2 consumption. They also reported that maximal vasodilation by papaverine decreased vascular wall O_2 consumption, which they attributed to a decrease in the smooth muscle workload (110). They did not consider whether there might have been greater NO production with an increase in shear stress as blood flow increased during vasodilation, and did not consider whether there might be effects of NO on O_2 consumption by the surrounding skeletal muscle in their preparation. A possible difference in vascular wall workload does not appear to explain the lower vascular wall O_2 consumption rate in eNOS-knockout mice found by Cabrales *et al.* (23). Since the arterial blood pressure was higher in the eNOS-knockout mice, the mechanical strain on the vascular walls of similar sized microvessels would be greater with a higher rate of vascular wall O_2 consumption than for the wild-type mice.

These apparently contradictory experimental findings might be resolved from predictive mathematical models for coupled NO and O_2 transport. However, many of the essential features and parameters for the different microcirculatory networks are not fully known. As an example of the difficulty in resolving this issue, Fig. 2 shows results for a computer model for convection and diffusion (similar to Refs. 27 and 28). The simulation is for a 30 μm internal diameter, 250 μm long

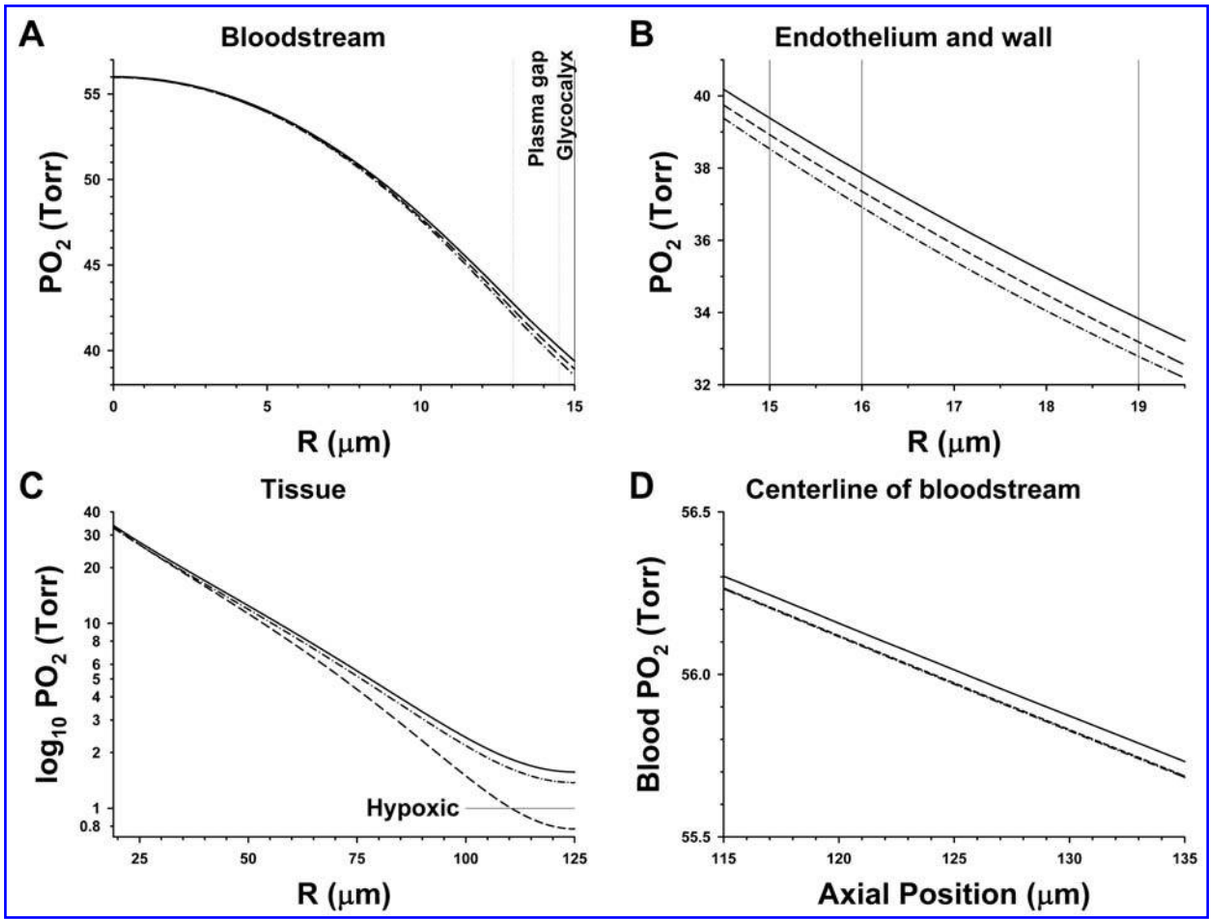

FIG. 2. Computer simulation for a convection and diffusion model of O_2 transport in cylindrical coordinates, showing predicted radial profiles for PO_2 in the bloodstream (A), endothelium and vascular wall (B), and tissue (C), with the longitudinal PO_2 gradient along the centerline of the bloodstream (D) at the midpoint of the arteriole for different O_2 consumption rates in the vascular wall and in tissue, with no NO present to inhibit O_2 consumption ($R_{NO} = 0$). The highest radial and longitudinal PO_2 profiles in each panel are for the baseline case with a low O_2 consumption rate for the vascular wall (see text for additional details).

arteriole using other parameters described in our previous models (19, 27, 28, 67–69). R_{NO} was set = 0 to eliminate effects of NO inhibition of O_2 consumption in this example. The concentric radial layers of the model (*inset at top* of Fig. 2) include a RBC-rich core at the center with a diameter of 26 μm and hematocrit of 45%, with thicknesses for the RBC-free plasma gap = 1.5 μm, glycocalyx = 0.5 μm, endothelium = 1 μm, and vascular wall = 3 μm. In this model, the glycocalyx serves as a stagnant layer with diffusion resistance, and other important functions, such as serving as a shear stress sensor to regulate endothelial NO release (see Ref. 43 for review) is not considered. The surrounding tissue receiving O_2 from this arteriole extended from 19 μm < R < 125 μm, with no contribution from capillaries or other sources of O_2 (zero mass flux at outer boundary). Blood flow through the arteriole was assumed to be constant at 33 nL min^{-1} with an ideal parabolic velocity profile having a maximum blood flow velocity (V_{max}) = 1 mm s^{-1} at the centerline (R = 0). The input PO_2 at the entrance of the arteriole was held constant at 60 Torr at the centerline.

The resulting computer simulation for O_2 transport is shown for three cases with different vascular wall and tissue O_2 consumption rates. Endothelial O_2 consumption was assumed to be negligible for this example, since production of NO was not included. The baseline case has a low O_2 consumption rate for the vascular wall = 1 μ*M* s^{-1} and a moderate O_2 consumption rate = 15 μ*M* s^{-1} in tissue, both with K_m = 1 Torr in the absence of NO (*solid curves* in Fig. 2A–D). Note that the simulation predicts a substantial radial PO_2 gradient in the bloodstream, shown for a cross-section located at the middle of the arteriolar segment length (Fig. 2A), due to diffusion out of the bloodstream to meet vascular wall and tissue O_2 demand. A similar, although somewhat blunter intraluminal radial PO_2 profile has been reported from high resolution O_2 phosphorescence quenching measurements in arterioles using a hamster skin fold window (13). Our convection and diffusion model for coupled NO and O_2 transport shows that the radial PO_2 profile becomes flatter when the velocity profile is blunter than the ideal parabolic shape (28).

Increasing the vascular wall O_2 consumption to a very high rate = 150 μ*M* s^{-1} (10 times higher than the tissue O_2 consumption rate) has only a small effect on the radial PO_2 gradient in blood and tissue (*dash–dot curves* in Fig. 2A–C). The

transmural PO_2 drop from the centerline to the outer vascular wall is 22.2 Torr for the baseline case, and only 1 Torr greater at 23.2 Torr with the considerably higher vascular wall O_2 consumption rate. There is a 1.75% steeper longitudinal PO_2 gradient = 2.90 Torr per 100 μm length of vessel (*lowest curve* in Fig. 2D), compared with the longitudinal PO_2 gradient = 2.85 Torr per 100 μm length of vessel for the baseline case. The effect of the high wall O_2 consumption rate on the amount of O_2 leaving the bloodstream is relatively minor for this example, since the volume of tissue in the vascular wall is small, only 0.7% of the volume for the surrounding tissue.

The third case (*dashed curves*, Fig. 2A–D) demonstrates that a similar change in the radial PO_2 profile can be made with only a 15% increase in tissue O_2 consumption to 18.25 $\mu M\ s^{-1}$ while keeping the vascular wall O_2 consumption low at 1 $\mu M\ s^{-1}$ (*dashed curves*, Fig. 2A–D). The longitudinal PO_2 gradient = 2.90 Torr per 100 μm length of vessel is identical to the high wall O_2 consumption case and the two curves overlap in Fig. 2D. However, the radial PO_2 gradient in tissue (*dashed curve*, Fig. 2C) falls to the lowest levels for this case, and deeper regions (R > 110.5 μm) are hypoxic with tissue PO_2 <1 Torr. Therefore, large variations in the vascular wall O_2 consumption rate have a much smaller effect on the radial PO_2 gradient, so that one would expect that smaller differences in tissue O_2 consumption rates will have a much greater influence on O_2 phosphorescence quenching measurements. This simulation is extended below to include NO production by eNOS and the effect of inhibition of O_2 consumption by NO.

ARE RBCS REALLY SUCH EFFICIENT SCAVENGERS OF NO?

The major route for elimination of NO is the reaction with oxygenated Hb to form MetHb and biologically inactive NO_3^-. As reviewed by Buerk (17), the rapid scavenging of NO found in studies with free Hb solutions was found to be somewhat problematic during initial efforts to mathematically model NO transport. The uptake of NO by Hb in RBCs was quickly recognized to be a critical parameter that had a profound effect on NO bioavailability in several early NO transport models (22, 71, 72, 76, 134, 135). Initially, it appeared that only a small fraction of the NO could escape scavenging reactions with Hb to reach the vascular wall. It was suggested that the rate of NO scavenging by RBCs must be diffusion limited. A similar concept had been shown from microvascular O_2 transport models, showing that diffusion barriers could limit the rate of O_2 release from RBCs (46). Several mathematical models have further investigated how diffusion barriers around the RBC and in the RBC-free plasma gap in the bloodstream near the endothelium can limit NO diffusion into the RBC (36, 54), including our own models that include coupled NO and O_2 transport (19, 27, 28, 67–69). However, it is still not clear how much NO must be produced by the endothelium to overcome the strong scavenging by Hb and be able to effectively control vascular tone.

In general, NO biotransport models have used hematocrit-dependent NO scavenging rates about 2 orders of magnitude less than scavenging rates for free Hb. This lower rate is still so rapid that downstream convective transport of NO can be neglected. For example, our simulations (19, 27, 28, 67–69) have been based on NO uptake rates measured with intact human RBCs by Carlsen and Comroe (24). More recently, Azarov *et al.* (5) evaluated the uptake of NO by RBCs under oxygenated and deoxygenated conditions, and report mean values of $3.6 \times 10^4\ M^{-1}s^{-1}$ when negligible amounts of methemoglobin (MetHb) are present, and $5.3 \times 10^4\ M^{-1}s^{-1}$ when significant amounts of MetHb are present to form MetHb-NO. In these studies, the uptake of NO by intact RBCs was slower by a factor of ~1,000 compared with free Hb, and about 21 times slower than found by Carlsen and Comroe (24) in their studies with intact RBCs. Azarov *et al.* (5) concluded that the rate of NO uptake by RBCs was primarily limited by diffusional barriers. They also found evidence that NO uptake depends on hematocrit and oxyhemoglobin saturation, so that deoxygenated RBCs scavenge NO faster than oxygenated RBCs. These aspects of O_2-dependent NO scavenging by RBCs have not as yet been addressed in mathematical models for coupled NO and O_2 transport in the microcirculation.

The computer simulation for convection and diffusion in a 30 μm internal diameter, 250 μm long arteriole shown previously in Fig. 2 was extended to include NO production by eNOS. The effects of the two different NO scavenging rates by RBCs on the simulation was compared, as shown in Fig. 3. The same dimensions and other parameters are used for the baseline case in Fig. 2, with $R_{NO} = 10\ \mu M\ s^{-1}$ by eNOS, similar to R_{NO} found with cultured endothelial cells. This adds an additional term for O_2 consumption by the endothelium at a rate = 20 $\mu M\ s^{-1}$ (two molecules of O_2 for each NO molecule produced) to the baseline case described previously, which is 33% higher than the tissue O_2 consumption rate used in the simulation. A first-order NO scavenging rate = 1 s^{-1} in endothelium, vascular wall, and tissue was assumed. Radial NO profiles with the 2 different NO scavenging rates by RBS are shown in Fig. 3A. There is no radial NO profile for the previous baseline case since there was zero NO production. For the value of R_{NO} used in this simulation, the peak NO value in the endothelium (Fig. 3A) is 21 n*M* for the higher NO scavenging rate by RBCs (24), and much higher at 63 n*M* for the lower NO scavenging rate (5). Note that there is a substantial amount of NO in the bloodstream for the lower NO scavenging rate by RBCs, with the blood NO = 47 n*M* at the centerline, compared with only 0.8 n*M* for the higher NO scavenging rate (Fig. 3A). This suggests that NO could be transported downstream by convection, where it would be free to diffuse out from capillaries or venules if the endothelial NO concentration is low (<47 n*M* for this example). Radial PO_2 profiles are plotted on a logarithmic scale in Fig. 3B, along with the previous baseline case without NO production (*solid curve*). With the NO scavenging rate for RBCs based on Carlsen and Comroe (24), O_2 consumption is inhibited more in the regions where NO levels are higher (*dash–dot curve*), with the net result that the radial PO_2 gradient (*dashed curve*) is higher than the baseline case (*solid curve*), causing higher PO_2 values at the outermost boundary. The lower NO scavenging rate by RBCs based on Azarov *et al.* (5) results in much higher NO levels (*dashed curve*, Fig. 3A) and greater inhibition of tissue O_2 consumption, causing an even greater increase in tissue PO_2 (*dashed curve*, Fig. 3B). The minimum PO_2 at R = 125 μm

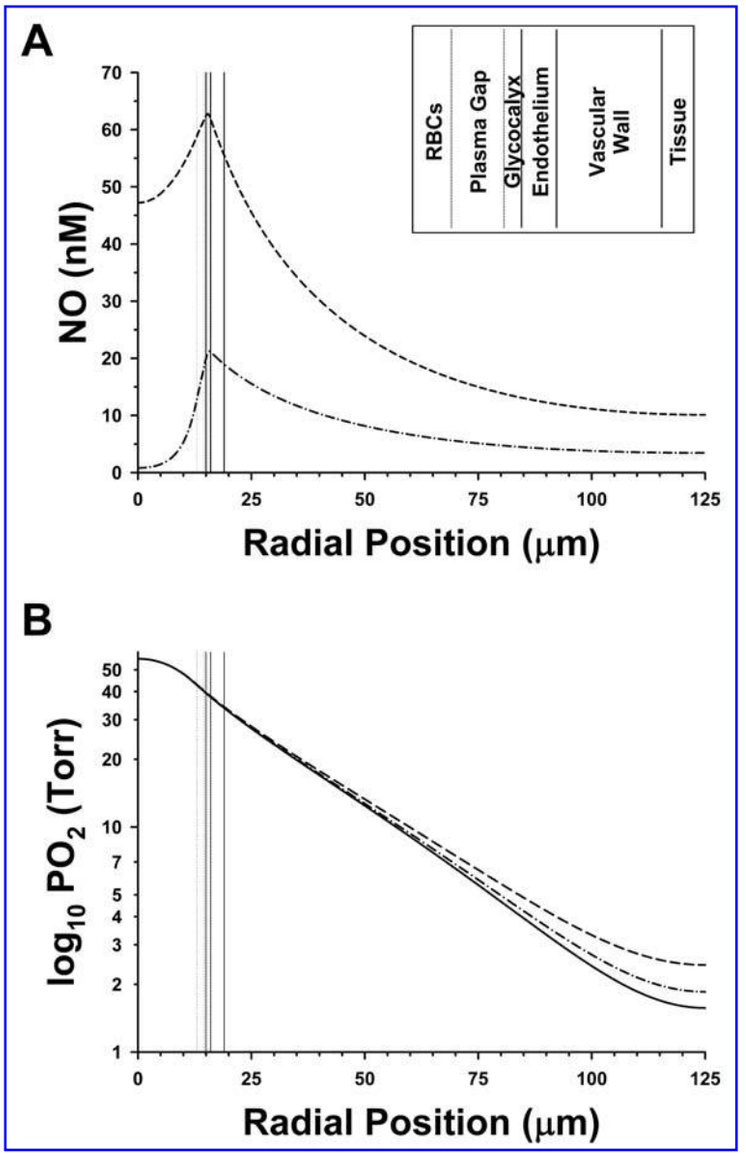

FIG. 3. Computer simulation for a convection and diffusion model of coupled O_2 and NO transport in cylindrical coordinates, showing predicted radial profiles for NO (A) and PO_2 (B) at the midpoint of a 30 μm diameter, 250 μm long arteriole for a parabolic blood flow velocity profile with V_{max} = 1 mm s^{-1} and endothelial R_{NO} = 10 μ*M* s^{-1} with NO scavenging rate for RBCs based on Carlsen and Comroe (24) (*dash-dot curves*) or lower NO scavenging rate based on Azorav *et al.*, (5) (*dashed curves*). Lowest PO_2 profile (*solid curve in **B***) is simulated for the previous baseline case (shown in Fig. 2) where there is no NO present to inhibit O_2 consumption (R_{NO} = 0). *Inset at top right* identifies the different concentric cylindrical layers in the model (see text for additional details).

is 1.57 Torr for the baseline case, and increases with NO production to 1.85 Torr with the higher NO scavenging rate for RBCs (24), and to 2.44 Torr with the lower rate (5). It should also be noted that a reduction in the tissue scavenging rate used in this simulation would also raise NO levels with a similar effect on increasing tissue PO_2 due to greater inhibition of O_2 consumption.

CAN SNO-HB CONSERVE NO?

Once NO reacts with Hb, it appears to be impossible for any free NO to diffuse out of the RBC. Azizi *et al.* (6) use the analogy that the RBC is a "black hole" for NO (*i.e.*, it can enter but cannot get out), based on their measurements of NO dissociation rates from Hb. While NO can slowly dissociate from Hb, it would then quickly react with the high concentration of Hb in the RBC. However, there is evidence for downstream transport of vasoactive species in the bloodstream that are apparently related to NO, for example with peripheral vasodilation following inhalation of low partial pressures of NO. It has been proposed that RBCs might be conserving appreciable amounts of NO by reacting with Hb to form SNO-Hb under oxygenated conditions, for subsequent downstream release of vasoactive products when O_2 tension in the bloodstream falls (see Ref. 113 for review). However, the experimental conditions for some previous studies in the literature have been questioned as to their physiological relevance. Angelo *et al.* (2) investigated NO_2^- and Hb interactions under what they felt were more physiological conditions, with cycles of oxygenation or deoxygenation and reoxygenation, allowing brief exposures of deoxygenated Hb or rapidly saturated oxygenated Hb to limiting levels of NO_2^-. They report that SNO-Hb was a major product, and that the amount of SNO-Hb produced was far greater than the amount of NO that can be predicted using published NO_2^- reduction rates.

A possible chemical reaction for the formation of SNO-Hb during the reduction of NO_2^- by deoxyhemoglobin has been proposed by Nagababu *et al.* (91). Doctor *et al.* (35) developed a sensitive and specific assay method which shows that elevated levels of SNO-Hb can be measured in venous blood samples in septic patients with systemic inflammatory response syndrome or with acute respiratory distress syndrome. Arterial blood samples from healthy volunteers were also analyzed. SNO-Hb in intact RBCs was found to be stable under oxygenated conditions, but declined as oxyhemoglobin saturation decreased.

ARE RBCS AND NITRITE COUPLED TO O_2 GRADIENTS IN THE MICROCIRCULATION?

The conservation of NO by SNO-Hb has been a controversial physiological mechanism and widely varying estimates for SNO-Hb concentrations in RBCs ranging from p*M* levels up to μ*M* levels have been reported. An alternative mechanism has been proposed where Hb in the RBC acts as an allosterically regulated NO_2^- reductase linked to O_2 gradients in the bloodstream (see Refs. 41 and 55 for reviews). Crawford *et al.* (30) reported that they were able to measure NO in the headspace above a suspension of RBCs by chemiluminescence methods as blood was deoxygenated, suggesting either that freely diffusible NO was able to escape the RBC "black hole" for NO, or that another intermediate species left the RBCs and was able to release NO that diffused out the fluid. As O_2 levels were reduced, they found greater vascular relaxation at lower concentrations of NO_2^-. They also demonstrated inhibition of mitochondrial respiration that was consistent with release of NO from RBCs in the presence of NO_2^-. In addition, they found evidence that ATP release from RBCs was a contributing factor in their studies, which might be regulated by NO. They report that the maximal NO_2^- reductase activity occurs at the P_{50} of the oxyhemoglobin equilibrium curve (OEC).

DOES NO ALTER THE OXYHEMOGLOBIN EQUILIBRIUM CURVE?

Evidence that NO shifts the affinity of the OEC for O_2 towards the right (increase in P_{50}) was reported a decade ago (60). A rightwards shift in OEC affinity would improve O_2 transport to tissue, since the blood PO_2 at a given saturation would be higher, with a larger concentration gradient for mass transport by diffusion. However, this has not been confirmed by more recent research. Zinchuk and Borisiuk (146) found that inhibition of NO production by L-NAME in rats caused a rightward shift in the OEC. Zinchuk and Dorokhina (147) also reported that L-arginine or the NO donor, sodium nitroprusside, administered intravenously to rats, shifted the OEC affinity for O_2 to the left. These two observations suggest that NO lowers the P_{50} of the OEC, which would decrease O_2 delivery to tissue by lowering the blood PO_2 at a given saturation. Consistent with these findings, Cabrales *et al.* (23) found that the OEC of eNOS knockout mice was shifted to the right (P_{50} = 48 Torr) compared with wild-type mice (P_{50} = 44 Torr). However, they found decreased intravascular and tissue PO_2 levels in the eNOS-knockout mice, most likely related to a higher tissue O_2 consumption compared with wild-type mice. This appears to have had a larger effect than any enhancement of O_2 delivery from a right-shifted OEC. More recently, Stepuro and Zinchuk (118) incubated rabbit blood with NO donors, L-arginine, or *S*-nitrosocysteine and evaluated changes in the OEC affinity for O_2. In this study, they found that *S*-nitrosocysteine shifted the OEC to the left, which they speculated may have been associated with formation of SNO-Hb. NO donors and L-arginine did not change the O_2 affinity of the OEC. Mechanisms that might cause a change in O_2 affinity with NO are not well characterized, and a precise relationship for the effect of NO on the P_{50} of the OEC has not yet been established.

BLOOD OXYGENATION AND CONTROL OF RESPIRATION

Blood oxygenation by the lungs depends on pulmonary blood flow, lung inflation volume, and the breathing rate. Blood oxygenation is sensed by the peripheral chemoreceptors, which send signals to respiratory centers in the lower brainstem to control respiration. The hypoxic ventilatory response is augmented in nNOS-knock mice (58), but blunted in eNOS-knockout mice (57), although it is difficult to separate out whether the response is due to effects of NO directly on the peripheral chemoreceptors and/or effects of NO on the lower brainstem respiratory centers. The carotid body chemoreceptors express both eNOS and nNOS, and NO inhibits the carotid body chemoreceptor response to hypoxia, as briefly reviewed by Lahiri *et al.* (66). Evidence that NO inhibits carotid body O_2 consumption was obtained from recessed PO_2 microelectrode measurements before and after inhibiting NO production (18, 65). On the other hand, NO appears to act as an excitatory neuromodulator of hypoxic ventilatory responses in the lower brainstem (see Ref. 39 for review). It has also been proposed that *S*-nitrosothiols carried to the nucleus tractus solitarius by the bloodstream causes an increase in neural activity that modulates the hypoxic ventilatory response (77).

VASCULAR ENDOTHELIAL GROWTH FACTOR AND ANGIOGENESIS

Adequate blood flow and O_2 delivery to tissue also requires maintenance and repair of the microcirculation through growth of new blood vessels. NO induces vascular endothelial growth factor (VEGF) expression in concert with reduced tissue O_2 levels and transcriptional activation of hypoxia-induced factor-1 (HIF-1) (52, 56, 99, 108, 131). Inhibition of NO production significantly reduces VEGF-induced angiogenesis (90, 144). Fukamura *et al.* (38) have shown that eNOS has a major role in angiogenesis from mouse cranial window studies of vascular growth in collagen

gels containing VEGF placed over the brain in wild-type and eNOS-knockout mice. Chronic lower limb ischemia studies with eNOS-knockout mice show impaired angiogenesis and pericyte recruitment that can be rescued by adenoviral gene delivery of an active allele of eNOS (141).

A BRIEF SURVEY OF SOME RELEVANT *IN VIVO* NO MEASUREMENTS

Several studies report values for perivascular NO levels in animals using NO microsensors with tips sufficiently small enough to obtain spatially localized measurements near the outer walls of microvessels in the microcirculation. The recessed, Nafion-coated NO microsensor developed by Buerk *et al.* (20), and used for studies in the eye, has the spatial and temporal resolution for these *in vivo* measurements. Perivascular NO concentrations are most likely to be lower than NO in the endothelium, based on the assumption that eNOS activity is the primary source for NO regulating microvascular tone. However, the NO measurements could also be influenced by NO produced from nNOS, mtNOS, or iNOS in the vascular wall, or if there is any stored NO released through alternative mechanisms, or by diffusion from adjacent venules or capillaries. Quantitative measurement of NO in the endothelium is not possible with NO microsensors, since the tip size exceeds endothelial dimensions. Also, the physical damage that would be caused by penetrating through the vascular wall is another limiting factor.

Experimental NO microsensor measurements of *in vivo* perivascular NO values are much higher than those shown for the simulation in Fig. 3, and in general, much higher than predicted by most mathematical models for NO transport in the literature, unless high values for R_{NO} are used. Bohlen (11) measured *in vivo* perivascular NO levels using recessed NO microsensors in a superfused rat mesentery and small intestine preparation, reporting mean ± SE values of 353 ± 28 n*M* around arterioles and 401 ± 48 n*M* around venules, and found that glucose absorption increased perivascular NO and caused vasodilation. Vukosavljevic *et al.* (137) measured similar NO levels in the same microcirculatory preparation, averaging 338 ± 40 n*M* around arterioles, with slightly lower values of 313 ± 48 n*M* around venules. In another study, Nase *et al.* (93) reported higher NO values averaging 522 ± 33 n*M* near arterioles with diameters averaging 53.2 ± 1.6 μm. Our direct *in vivo* measurements of perivascular NO directly confirmed that excess L-arginine caused a significant increase in NO and an increase in tissue perfusion after superfusing the preparation for several minutes (137). We found a doubling of perivascular NO for the conditions of our study using a concentration of ~100 μ*M* for excess L-arginine in the superfusate. Although we found that venules had a slightly larger increase in NO increase with excess L-arginine compared to arterioles, we did not find any statistical significance between vessel type for either the baseline NO or the response to L-arginine. Some of our findings are similar to an earlier study by Bohlen (11), who measured changes in NO after continuous topical administration of 1 m*M* L-arginine and reported a two-fold increase in NO after L-arginine administration from a baseline of 334 ± 19 to 686 ± 53 n*M* within 2–3 min. Using the amino acid L-lysine to compete with L-arginine transport via CAAT, Zani and Bohlen (142) found decreased NO production and blood flow in rat intestinal arterioles. Also, L-lysine suppressed expected increases in NO and blood flow during hypoxia and with NaCl hyperosmolarity.

Tsai *et al.* (129) report even higher perivascular NO values averaging 632 ± 36 n*M* for arterioles with average diameter of 54.9 ± 17.7 μm and venules with average diameter of 61.9 ± 18.3 μm in the skinfold of conscious hamsters using a bare carbon fiber tip NO microsensor coated with Nafion. There was no appreciable difference between the perivascular NO values for arterioles and venules. In this study, NO measurements were repeated at different perivascular locations after the animals were exchange transfused using Dextran solutions with either high or low viscosity, reducing hematocrit by about one fourth, from 45% to 11% in both cases. There were no significant changes in arteriolar or venular diameters after transfusion, but significant differences in microvascular hemodynamics were found which depended on the final microvascular viscosities. RBC velocity and calculated flow rates were significantly lower in both arterioles and venules for the low viscosity transfusion compared to the control state before hemodilution. The opposite result was found for the high viscosity transfusion, with significant increases in red blood cell velocity and calculated flow, especially for the venules. Interestingly, NO levels were higher for both arterioles and venules after transfusion with the high viscosity solution. In contrast, a reduction in perivascular NO levels was seen after transfusion with a low viscosity solution. The first observation is consistent with a reduction in NO scavenging by hemoglobin, but the second observation is not consistent with this explanation. Wall shear stresses were calculated for the control and hemodiluted conditions, and were higher for the high viscosity transfusion compared with the low viscosity transfusion, but no significant statistical relationship was found between shear stress and perivascular NO levels.

In another *in vivo* NO microelectrode study, Palm *et al.* (98) report that intravenous injections of L-arginine caused an increase in renal tissue NO in normal rats, but a smaller NO response in streptozotocin (STZ)-induced diabetic rats. Our study suggests that the smaller NO response to excess L-arginine in STZ-induced diabetic rats is likely due to a reduction in L-arginine availability, which we found to be 38% lower compared to control rats.

Very high baseline tissue NO levels (>2 μ*M*) have been measured in tumors implanted in immunodeficient mice (53), which are related to NO production by eNOS and are higher with increasing density of blood vessels, as illustrated in Fig. 4. In Fig. 4A, NO profiles are shown as a recessed NO microsensor (indicated by *arrows* in cranial window images) was slowly moved at a constant microdrive rate from the artificial cerebral spinal fluid superfusing the brain surface in the open cranial window, and advanced either into the cerebral cortex (*left panels*) or into a nearby melanoma tumor with a high metastatic potential (B16F10) that had been implanted in the cranial window (*right panels*) ~1 week prior to the study. Similar NO profiles were measured in melanoma tumors with low metastatic potential (B16F1) implanted in cranial windows, and in dorsal skin chambers with implanted

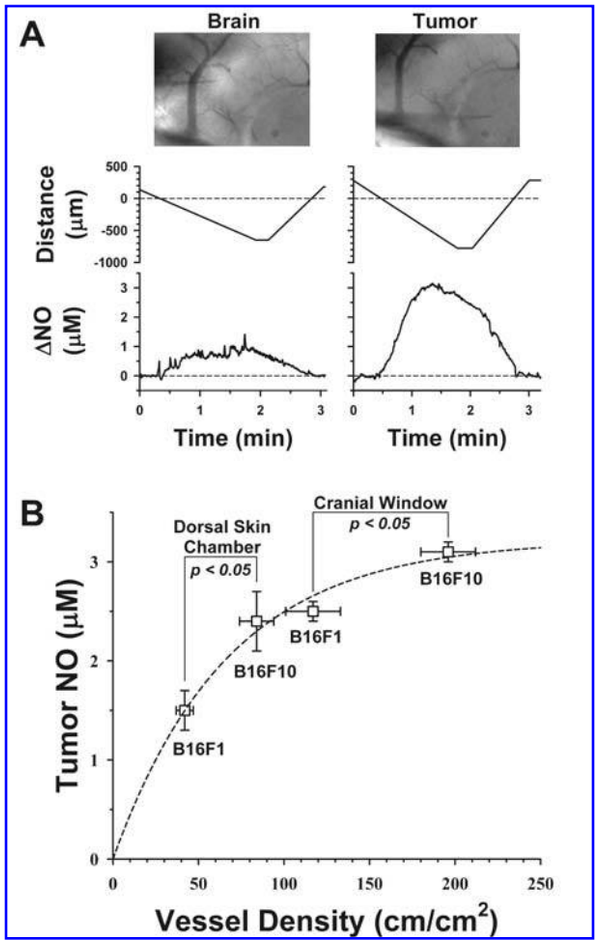

FIG. 4. Recessed NO microelectrode measurements (**A**) in cerebral cortex (*left panels*) and in a melanoma tumor (*right panels*) grown in a cranial window, and (**B**) the nonlinear relationship between average NO and vascular density for melanoma tumors with high (B16F10) or low (B16F1) metastatic potential implanted in cranial windows or dorsal skin chambers in immunodeficient mice [data from Kashiwagi *et al.* (53)]. *Arrows* in cranial window images indicate location of the NO microelectrode.

melanoma tumors that had either high or low metastatic potential. The nonlinear relationship between the mean ± SE NO and vascular density is plotted in Fig. 4B from the data in Table 1 of Kashiwagi *et al.* (53). The average NO levels were higher in melanoma tumors grown in cranial windows compared with dorsal skin windows, and in each case, NO was higher in the melanoma tumors with higher metastatic potential.

NO profiles were measured with recessed NO microsensors across collagen gels containing VEGF implanted in cranial windows in wild-type mice and eNOS-knockout mice (38). Much higher NO levels were found in the studies with wild-type mice. Growth of new vessels in the collagen gel was slower in the eNOS-knockout mice with a lower density of vessels compared with wild-type mice. An inhibitor of iNOS had little effect on angiogenesis or on NO levels in either wild-type or eNOS-knockout studies.

In another *in vivo* NO microsensor study in rat brain, Thom *et al.* (126) found that a two-stage exposure to low levels of CO for 1 h, starting at 1,000 ppm for 40 min, then 3,000 pp for 20 min, caused NO to increase by almost twofold over baseline levels. Mean ± SE baseline NO levels in the cerebral cortex prior to CO exposure were 297 ± 93 n*M*, based on the decrease in measured NO following L-NAME in four rats from this study. The increase in NO was associated with activation of nNOS due to the effects of CO on *N*-methyl-D-aspartate (NMDA) receptors. The increase in NO with CO exposure could be partially blocked with 7-nitroindazole, a nNOS inhibitor, and by a NDMA receptor agonist.

Very large increases in NO from baseline have been measured with recessed NO microsensors during exposure to hyperbaric O_2 in rodent brain (123, 125), at perivascular sites in rodents (127), and in bone marrow in mice (42, 124). While the O_2-dependent production of NO by different NOS isoforms may account for most of this response, we also found evidence that oxidative stress mechanisms were involved in activating NOS. Thom *et al.* (123) found that intravenous infusion of the antioxidant agents SOD or *N*-acetylcysteine attenuated the increase in NO with hyperbaric O_2 in the rodent brain. Evidence for NOS activation due to an increase in heat shock protein 90 during hyperbaric O_2 was also found. Studies with wild-type, eNOS-, and nNOS-knockout mice demonstrated that the increase in NO was mainly due to an increase in nNOS activity, which could be nearly completely blocked with 7-nitroindazole, an inhibitor of nNOS (123). Simultaneous PO_2 and NO measurements from perivascular sites in rats demonstrated that the increase in NO during hyperbaric O_2 lagged behind the increase in O_2 (127). The magnitude of the increase in NO depended on the degree of hyperbaric exposure, which was studied up to 2.8 atmospheres. The NO response could be blocked with the general NOS inhibitor L-NAME, and was also significantly reduced with the nNOS inhibitor 7-nitroindazole. Inhibitors of iNOS had no effect. Studies with wild-type, eNOS-knockout, and nNOS-knockout mice were also done, showing little difference in the NO response for wild-type and eNOS-knockout mice, but a much smaller NO response for the nNOS-knockout mice (127).

Studies in humans and mice (42, 124) found that hyperbaric O_2 lead to an increase in circulating endothelial progenitor cells, more so after exposure to 2.4 or 2.8 atmospheres than for lower hyperbaric pressures below 2 atmospheres. In both studies, large increases in NO above baseline were measured in the marrow of the femoral bone in mice during hyperbaric O_2 exposure. Studies with eNOS-knockout mice demonstrated that there was no increase in circulating endothelial progenitor cells after hyperbaric O_2 (124). In studies of wound healing in mice with an ischemic hind limb created by femoral ligation, with the unaltered opposite limb serving as a control (42), hyperbaric O_2 lead to the reestablishment of blood flow to the ischemic limb, with an increase in migration of circulating endothelial progenitor cells to the ischemic tissue, and an accelerated rate of wound healing. The rise in bone marrow NO could be essentially eliminated with L-NAME. Mice that received L-NAME did not reestablish blood flow to the ischemic limb, which developed distal gangrene resulting in the loss of tissue, even with hyperbaric O_2 treatment.

SUMMARY

There are many factors that should be incorporated into mathematical models for coupled NO and O_2 transport if quantitative relationships can be formulated. These modifications might include the many factors that influence NOS activity, the effects of NO binding at different catalytic sites on activation of sGC, inclusion of other vasoactive NO-related species that might be formed by reactions with Hb and transported downstream in the bloodstream, more complex relationships for the inhibition of O_2 consumption by NO including effects at different sites on cytochrome *c* oxidase, and interactions with other oxidases that generate O_2^-. Of course, experimental studies would be required to validate whether these predictive models are physiologically relevant. However, the limited number of *in vivo* measurements of NO in different experimental studies suggests that NO levels are higher than has been generally believed, and our understanding of the mechanisms for generating and removing NO in biological systems needs to be examined in light of these observations.

ACKNOWLEDGMENTS

Research with NO microsensors was supported in part by NIH (HL 068164, EY 09269, AT 00428) and NSF (BES 0301446).

ABBREVIATIONS

ADMA, asymmetric dimethylarginine; ATP, adenosine 5′-triphosphate; BH_2, oxidized tetrahydropterin; BH_4, tetrahydropterin; Ca^{2+}, calcium ion; CAAT, cationic amino acid transporter; cGMP, 3',5′-cyclic guanosine monophosphate; CO, carbon monoxide; CO_2, carbon dioxide; CO_3^-, carbonate ion; COX, cyclooxygenase; DAF, diaminofluorescein; eNOS, endothelial isoform of NOS; GSH, glutathione; GSNO, *S*-nitrosoglutathione; GTPCH, guanidine triphosphate cyclohydrolase; Hb, hemoglobin; HO, heme oxygenase; H_2S, hydrogen sulfide; HIF-1, hypoxia-inducible factor-1; iNOS, inducible isoform of NOS; K_m, Michaelis–Menten constant; L-NAME, N^{ω}-nitro-L-arginine methyl ester; Mb, myoglobin; MetHb, methemoglobin; MetHb-NO, nitrosylhemoglobin; mtNOS, mitochondrial isoform of NOS; NADPH, nicotinamide-adenine-dinucleotide phosphate; NMDA , *N*-methyl-D-aspartate; nNOS, neuronal isoform of NOS; NO, nitric oxide; NO_2, nitrogen dioxide; NO_2^-, nitrite; NO_3^-, nitrate; N_2O_3, nitrous anhydride; NOHA, N^G-hydroxy-L-arginine; O_2, oxygen; O_2^-, superoxide; OEC, oxyhemoglobin equilibrium curve; $ONOO^-$, peroxynitrite; PO_2, O_2 partial pressure; ppm, parts per million; P_{50}, PO_2 where oxyhemoglobin equilibrium curve is 50% saturated; R, radius; RBC, red blood cell; ROS, reactive oxygen species; R_{NO}, NO production rate; RNS, reactive nitrogen species; sGC, soluble guanylate cyclase; SNO-Hb, *S*-nitrosohemoglobin; SOD, superoxide dismutase; STZ, streptozotocin; VEGF, vascular endothelial growth factor; V_{max}, maximum blood flow velocity.

REFERENCES

1. Alvarez S, Valdez LB, Zaobornyj T, and Boveris A. Oxygen dependence of mitochondrial nitric oxide synthase activity. *Biochem Biophys Res Commun* 305: 771–775, 2003.
2. Angelo M, Singel DJ, and Stamler JS. An *S*-nitrosothiol (SNO) synthase function of hemoglobin that utilizes nitrite as a substrate. *Proc Natl Acad Sci USA* 103: 8366–8371, 2006.
3. Antunes F, Boveris A, and Cadenas E. On the mechanism and biology of cytochrome oxidase inhibition by nitric oxide. *Proc Natl Acad Sci USA* 101: 16774–16779, 2004.
4. Arnal JF, Munzel T, Venema RC, James NL, Bai CL, Mitch WE, and Harrison DG. Interactions between *L*-arginine and *L*-glutamine change endothelial NO production. An effect independent of NO synthase substrate availability. *J Clin Invest* 95: 2565–2572, 1995.
5. Azarov I, Huang KT, Basu S, Gladwin MT, Hogg N, and Kim–Shapiro DB. Nitric oxide scavenging by red blood cells as a function of hematocrit and oxygenation. *J Biol Chem* 280: 39024–39032, 2005.
6. Azizi F, Kielbasa JE, Adeyiga AM, Maree RD, Frazier M, Yakubu M, Shields H, King SB, and Kim–Shapiro DB. Rates of nitric oxide dissociation from hemoglobin. *Free Radic Biol Med* 39: 145–151, 2005.
7. Bergfeld GR and Forrester T. Release of ATP from human erythrocytes in response to a brief period of hypoxia and hypercapnia. *Cardiovasc Res* 26: 40–47, 1992.
8. Bivalacqua TJ, Hellstrom WJ, Kadowitz PJ, and Champion HC. Increased expression of arginase II in human diabetic corpus cavernosum: in diabetic-associated erectile dysfunction. *Biochem Biophys Res Commun* 283: 923–927, 2001.
9. Boger RH. Asymmetric dimethylarginine (ADMA) and cardiovascular disease: insights from prospective clinical trials. *Vasc Med* 10 (Suppl 1): S19–25, 2005.
10. Bogle RG, Baydoun AR, Pearson JD, and Mann GE. Regulation of L-arginine transport and nitric oxide release in superfused porcine aortic endothelial cells. *J Physiol* 490: 229–241, 1996.
11. Bohlen HG. Mechanism of increased vessel wall nitric oxide concentrations during intestinal absorption. *Am J Physiol* 275: H542–550, 1998.
12. Boon EM, Huang SH, and Marletta MA. A molecular basis for NO selectivity in soluble guanylate cyclase. *Nat Chem Biol* 1: 53–59, 2005.
13. Briceno JC, Cabrales P, Tsai AG, and Intaglietta M. Radial displacement of red blood cells during hemodilution and the effect on arteriolar oxygen profile. *Am J Physiol Heart Circ Physiol* 286: H1223–1228, 2004.
14. Brown GC and Cooper CE. Nanomolar concentrations of nitric oxide reversibly inhibit synaptosomal respiration by competing with oxygen at cytochrome oxidase. *FEBS Lett* 356: 295–298, 1994.
15. Brunori M, Giuffre A, Nienhaus K, Nienhaus GU, Scandurra FM, and Vallone B. Neuroglobin, nitric oxide, and oxygen: functional pathways and conformational changes. *Proc Natl Acad Sci USA* 102: 8483–8488, 2005.
16. Bryan NS. Nitrite in nitric oxide biology: cause or consequence? A systems-based review. *Free Radic Biol Med* 41: 691–701, 2006.
17. Buerk DG. Can we model nitric oxide biotransport? A survey of mathematical models for a simple diatomic molecule with surprisingly complex biological activities. *Annu Rev Biomed Eng* 3: 109–143, 2001.
18. Buerk DG and Lahiri S. Evidence that nitric oxide plays a role in O_2 sensing from tissue NO and PO_2 measurements in cat carotid body. *Adv Exp Med Biol* 475: 337–347, 2000.
19. Buerk DG, Lamkin–Kennard K, and Jaron D. Modeling the influence of superoxide dismutase on superoxide and nitric oxide interactions, including reversible inhibition of oxygen consumption. *Free Radic Biol Med* 34: 1488–1503, 2003.
20. Buerk DG, Riva CE, and Cranstoun SD. Nitric oxide has a vasodilatory role in cat optic nerve head during flicker stimuli. *Microvasc Res* 52: 13–26, 1996.
21. Buga GM, Singh R, Pervin S, Rogers NE, Schmitz DA, Jenkinson CP, Cederbaum SD, and Ignarro LJ. Arginase activity

in endothelial cells: inhibition by N^G-hydroxy-*L*-arginine during high-output NO production. *Am J Physiol* 271: H1988–1998, 1996.
22. Butler AR, Megson IL, and Wright PG. Diffusion of nitric oxide and scavenging by blood in vasculature. *Biochim Biophys Acta* 1425: 168–176, 1998.
23. Cabrales P, Tsai AG, Frangos JA, and Intaglietta M. Role of endothelial nitric oxide in microvascular oxygen delivery and consumption. *Free Radic Biol Med* 39: 1229–1237, 2005.
24. Carlsen E and Comroe JHJ. The rate of uptake of carbon monoxide and of nitric oxide by normal human erythrocytes and experimentally produced spherocytes. *J Gen Physiol* 42: 83–107, 1958.
25. Cary SP, Winger JA, Derbyshire ER, and Marletta MA. Nitric oxide signaling: no longer simply on or off. *Trends Biochem Sci* 31: 231–239, 2006.
26. Chen K and Popel AS. Theoretical analysis of biochemical pathways of nitric oxide release from vascular endothelial cells. *Free Radic Biol Med* 41: 668–680, 2006.
27. Chen X, Buerk DG, Barbee KA, and Jaron D. A model of NO/O_2 transport in capillary-perfused tissue containing an arteriole and venule pair. *Ann Biomed Eng* 35: 517–529, 2007.
28. Chen X, Jaron D, Barbee KA, and Buerk DG. The influence of radial RBC distribution, blood velocity profiles, and glycocalyx on coupled NO/O_2 transport. *J Appl Physiol* 100: 482–492, 2006.
29. Cleeter MW, Cooper JM, Darley–Usmar VM, Moncada S, and Schapira AH. Reversible inhibition of cytochrome *c* oxidase, the terminal enzyme of the mitochondrial respiratory chain, by nitric oxide. Implications for neurodegenerative diseases. *FEBS Lett* 345: 50–54, 1994.
30. Crawford JH, Isbell TS, Huang Z, Shiva S, Chacko BK, Schechter AN, Darley-Usmar VM, Kerby JD, Lang JD, Jr., Kraus D, Ho C, Gladwin MT, and Patel RP. Hypoxia, red blood cells, and nitrite regulate NO-dependent hypoxic vasodilation. *Blood* 107: 566–574, 2006.
31. Csordas A, Pankotai E, Snipes JA, Cselenyak A, Sarszegi Z, Cziraki A, Gaszner B, Papp L, Benko R, Kiss L, Kovacs E, Kollai M, Szabo C, Busija DW, and Lacza Z. Human heart mitochondria do not produce physiologically relevant quantities of nitric oxide. *Life Sci* 80: 633–637, 2007 In Press.
32. Demougeot C, Prigent–Tessier A, Marie C, and Berthelot A. Arginase inhibition reduces endothelial dysfunction and blood pressure rising in spontaneously hypertensive rats. *J Hypertens* 23: 971–978, 2005.
33. Denninger JW and Marletta MA. Guanylate cyclase and the .NO/cGMP signaling pathway. *Biochim Biophys Acta* 1411: 334–350, 1999.
34. Dhanakoti SN, Brosnan JT, Herzberg GR, and Brosnan ME. Renal arginine synthesis: studies *in vitro* and *in vivo*. *Am J Physiol* 259: E437–442, 1990.
35. Doctor A, Platt R, Sheram ML, Eischeid A, McMahon T, Maxey T, Doherty J, Axelrod M, Kline J, Gurka M, Gow A, and Gaston B. Hemoglobin conformation couples erythrocyte *S*-nitrosothiol content to O_2 gradients. *Proc Natl Acad Sci USA* 102: 5709–5714, 2005.
36. El–Farra NH, Christofides PD, and Liao JC. Analysis of nitric oxide consumption by erythrocytes in blood vessels using a distributed multicellular model. *Ann Biomed Eng* 31: 294–309, 2003.
37. Ellsworth ML, Forrester T, Ellis CG, and Dietrich HH. The erythrocyte as a regulator of vascular tone. *Am J Physiol* 269: H2155–2161, 1995.
38. Fukumura D, Gohongi T, Kadambi A, Izumi Y, Ang J, Yun CO, Buerk DG, Huang PL, and Jain RK. Predominant role of endothelial nitric oxide synthase in vascular endothelial growth factor-induced angiogenesis and vascular permeability. *Proc Natl Acad Sci USA* 98: 2604–2609, 2001.
39. Gaston B, Singel D, Doctor A, and Stamler JS. *S*-nitrosothiol signaling in respiratory biology. *Am J Respir Crit Care Med* 173: 1186–1193, 2006.
40. Giulivi C, Kato K, and Cooper CE. Nitric oxide regulation of mitochondrial oxygen consumption I: cellular physiology. *Am J Physiol Cell Physiol* 291: C1225–1231, 2006.
41. Gladwin MT, Raat NJ, Shiva S, Dezfulian C, Hogg N, Kim–Shapiro DB, and Patel RP. Nitrite as a vascular endocrine nitric oxide reservoir that contributes to hypoxic signaling, cytoprotection, and vasodilation. *Am J Physiol Heart Circ Physiol* 291: H2026–2035, 2006.
42. Goldstein LJ, Gallagher KA, Bauer SM, Bauer RJ, Baireddy V, Liu ZJ, Buerk DG, Thom SR, and Velazquez OC. Endothelial progenitor cell release into circulation is triggered by hyperoxia-induced increases in bone marrow nitric oxide. *Stem Cells* 24: 2309–2318, 2006.
43. Gouverneur M, Berg B, Nieuwdorp M, Stroes E, and Vink H. Vasculoprotective properties of the endothelial glycocalyx: effects of fluid shear stress. *J Intern Med* 259: 393–400, 2006.
44. Gow AJ, Buerk DG, and Ischiropoulos H. A novel reaction mechanism for the formation of *S*-nitrosothiol *in vivo*. *J Biol Chem* 272: 2841–2845, 1997.
45. Handy DE, and Loscalzo J. Nitric oxide and posttranslational modification of the vascular proteome: *S*-nitrosation of reactive thiols. *Arterioscler Thromb Vasc Biol* 26: 1207–1214, 2006.
46. Hellums JD, Nair PK, Huang NS, and Ohshima N. Simulation of intraluminal gas transport processes in the microcirculation. *Ann Biomed Eng* 24: 1–24, 1996.
47. Huang PL, Dawson TM, Bredt DS, Snyder SH, and Fishman MC. Targeted disruption of the neuronal nitric oxide synthase gene. *Cell* 75: 1273–1286, 1993.
48. Huang PL, Huang Z, Mashimo H, Bloch KD, Moskowitz MA, Bevan JA, and Fishman MC. Hypertension in mice lacking the gene for endothelial nitric oxide synthase. *Nature* 377: 239–242, 1995.
49. Huynh NN and Chin–Dusting J. Amino acids, arginase and nitric oxide in vascular health. *Clin Exp Pharmacol Physiol* 33: 1–8, 2006.
50. Ignarro LJ, Buga GM, Wood KS, Byrns RE, and Chaudhuri G. Endothelium-derived relaxing factor produced and released from artery and vein is nitric oxide. *Proc Natl Acad Sci USA* 84: 9265–9269, 1987.
51. Johnson FK, Johnson RA, Peyton KJ, and Durante W. Arginase inhibition restores arteriolar endothelial function in Dahl rats with salt-induced hypertension. *Am J Physiol Regul Integr Comp Physiol* 288: R1057–1062, 2005.
52. Jozkowicz A, Cooke JP, Guevara I, Huk I, Funovics P, Pachinger O, Weidinger F, and Dulak J. Genetic augmentation of nitric oxide synthase increases the vascular generation of VEGF. *Cardiovasc Res* 51: 773–783, 2001.
53. Kashiwagi S, Izumi Y, Gohongi T, Demou ZN, Xu L, Huang PL, Buerk DG, Munn LL, Jain RK, and Fukumura D. NO mediates mural cell recruitment and vessel morphogenesis in murine melanomas and tissue-engineered blood vessels *J Clin Invest* 115: 1816–1837, 2005.
54. Kavdia M, Tsoukias NM, and Popel AS. Model of nitric oxide diffusion in an arteriole: impact of hemoglobin-based blood substitutes *Am J Physiol Heart Circ Physiol* 282: H2245–2253, 2002.
55. Kim–Shapiro DB, Schechter AN, and Gladwin MT. Unraveling the reactions of nitric oxide, nitrite, and hemoglobin in physiology and therapeutics. *Arterioscler Thromb Vasc Biol* 26: 697–705, 2006.
56. Kimura H, Weisz A, Ogura T, Hitomi Y, Kurashima Y, Hashimoto K, D'Acquisto F, Makuuchi M, and Esumi H. Identification of hypoxia-inducible factor 1 ancillary sequence and its function in vascular endothelial growth factor gene induction by hypoxia and nitric oxide. *J Biol Chem* 276: 2292–2298, 2001.
57. Kline DD and Prabhakar NR. Peripheral chemosensitivity in mutant mice deficient in nitric oxide synthase. *Adv Exp Med Biol* 475: 571–579, 2000.
58. Kline DD, Yang T, Huang PL, and Prabhakar NR. Altered respiratory responses to hypoxia in mutant mice deficient in neuronal nitric oxide synthase. *J Physiol* 511: 273–287, 1998.
59. Koivisto A, Matthias A, Bronnikov G, and Nedergaard J. Kinetics of the inhibition of mitochondrial respiration by NO. *FEBS Lett* 417: 75–80, 1997.
60. Kosaka H and Seiyama A. Physiological role of nitric oxide as an enhancer of oxygen transfer from erythrocytes to tissues. *Biochem Biophys Res Commun* 218: 749–752, 1996.

61. Kuchan MJ and Frangos JA. Role of calcium and calmodulin in flow-induced nitric oxide production in endothelial cells. *Am J Physiol* 266: C628–636, 1994.
62. Kurz S and Harrison DG. Insulin and the arginine paradox. *J Clin Invest* 99: 369–370, 1997.
63. Kuzkaya N, Weissmann N, Harrison DG, and Dikalov S. Interactions of peroxynitrite, tetrahydrobiopterin, ascorbic acid, and thiols: implications for uncoupling endothelial nitric-oxide synthase. *J Biol Chem* 278: 22546–22554, 2003.
64. Lacza Z, Pankotai E, Csordas A, Gero D, Kiss L, Horvath EM, Kollai M, Busija DW, and Szabo C. Mitochondrial NO and reactive nitrogen species production: does mtNOS exist? *Nitric Oxide* 14: 162–168, 2006.
65. Lahiri S and Buerk DG. Vascular and metabolic effects of nitric oxide synthase inhibition evaluated by tissue PO_2 measurements in carotid body. *Adv Exp Med Biol* 454: 455–460, 1998.
66. Lahiri S, Rozanov C, Roy A, Storey B, and Buerk DG. Regulation of oxygen sensing in peripheral arterial chemoreceptors. *Int J Biochem Cell Biol* 33: 755–774, 2001.
67. Lamkin–Kennard K, Jaron D, and Buerk DG. Modeling the regulation of oxygen consumption by nitric oxide. *Adv Exp Med Biol* 510: 145–159, 2003.
68. Lamkin–Kennard KA, Buerk DG, and Jaron D. Interactions between NO and O_2 in the microcirculation: a mathematical analysis. *Microvasc Res* 68: 38–50, 2004.
69. Lamkin–Kennard KA, Jaron D, and Buerk DG. Impact of the Fåhraeus effect on NO and O_2 biotransport: a computer model. *Microcirculation* 11: 337–349, 2004.
70. Lancaster JR, Jr. Nitroxidative, nitrosative, and nitrative stress: kinetic predictions of reactive nitrogen species chemistry under biological conditions. *Chem Res Toxicol* 19: 1160–1174, 2006.
71. Lancaster JR, Jr. Simulation of the diffusion and reaction of endogenously produced nitric oxide. *Proc Natl Acad Sci USA* 91: 8137–8141, 1994.
72. Lancaster JR, Jr. A tutorial on the diffusibility and reactivity of free nitric oxide. *Nitric Oxide* 1: 18–30, 1997.
73. Landmesser U, Harrison DG, and Drexler H. Oxidant stress-a major cause of reduced endothelial nitric oxide availability in cardiovascular disease. *Eur J Clin Pharmacol* 62: 13–19, 2006.
74. Lass A, Suessenbacher A, Wolkart G, Mayer B, and Brunner F. Functional and analytical evidence for scavenging of oxygen radicals by L-arginine. *Mol Pharmacol* 61: 1081–1088, 2002.
75. Lee Y, Yang J, Rudich SM, Schreiner RJ, and Meyerhoff ME. Improved planar amperometric nitric oxide sensor based on platinized platinum anode. 2. Direct real-time measurement of NO generated from porcine kidney slices in the presence of l-arginine, l-arginine polymers, and protamine. *Anal Chem* 76: 545–551, 2004.
76. Liao JC, Hein TW, Vaughn MW, Huang KT, and Kuo L. Intravascular flow decreases erythrocyte consumption of nitric oxide. *Proc Natl Acad Sci USA* 96: 8757–8761, 1999.
77. Lipton AJ, Johnson MA, Macdonald T, Lieberman MW, Gozal D, and Gaston B. S-nitrosothiols signal the ventilatory response to hypoxia. *Nature* 413: 171–174, 2001.
78. Lu X and Kassab GS. Nitric oxide is significantly reduced in ex vivo porcine arteries during reverse flow because of increased superoxide production. *J Physiol* 561: 575–582, 2004.
79. Malinski T, Taha Z, Grunfeld S, Patton S, Kapturczak M, and Tomboulian P. Diffusion of nitric oxide in the aorta wall monitored in situ by porphyrinic microsensors. *Biochem Biophys Res Commun* 193: 1076–1082, 1993.
80. Mason MG, Nicholls P, Wilson MT, and Cooper CE. Nitric oxide inhibition of respiration involves both competitive (heme) and noncompetitive (copper) binding to cytochrome *c* oxidase. *Proc Natl Acad Sci USA* 103: 708–713, 2006.
81. McDonald KK, Zharikov S, Block ER, and Kilberg MS. A caveolar complex between the cationic amino acid transporter 1 and endothelial nitric-oxide synthase may explain the "arginine paradox." *J Biol Chem* 272: 31213–31216, 1997.
82. Meurs H, Maarsingh H, and Zaagsma J. Arginase and asthma: novel insights into nitric oxide homeostasis and airway hyperresponsiveness. *Trends Pharmacol Sci* 24: 450–455, 2003.
83. Milstien S and Katusic Z. Oxidation of tetrahydrobiopterin by peroxynitrite: implications for vascular endothelial function. *Biochem Biophys Res Commun* 263: 681–684, 1999.
84. Ming XF, Barandier C, Viswambharan H, Kwak BR, Mach F, Mazzolai L, Hayoz D, Ruffieux J, Rusconi S, Montani JP, and Yang Z. Thrombin stimulates human endothelial arginase enzymatic activity via RhoA/ROCK pathway: implications for atherosclerotic endothelial dysfunction. *Circulation* 110: 3708–3714, 2004.
85. Mittermayer F, Krzyzanowska K, Exner M, Mlekusch W, Amighi J, Sabeti S, Minar E, Muller M, Wolzt M, and Schillinger M. Asymmetric dimethylarginine predicts major adverse cardiovascular events in patients with advanced peripheral artery disease. *Arterioscler Thromb Vasc Biol* 26: 2536–2540, 2006.
86. Moens AL and Kass DA. Tetrahydrobiopterin and cardiovascular disease. *Arterioscler Thromb Vasc Biol* 26: 2439–2444, 2006.
87. Moncada S and Higgs EA. The discovery of nitric oxide and its role in vascular biology. *Br J Pharmacol* 147 (Suppl 1): S193–201, 2006.
88. Moncada S, Palmer RMJ, and Higgs EA. Nitric-oxide–Physiology, pathophysiology, and pharmacology. *Pharmacol Rev* 43: 109–142, 1991.
89. Morris SMJ. Enzymes of arginine metabolism *J Nutr* 134: 2743S–2747S, 2004.
90. Murohara T, Horowitz JR, Silver M, Tsurumi Y, Chen D, Sullivan A, and Isner JM. Vascular endothelial growth factor/vascular permeability factor enhances vascular permeability via nitric oxide and prostacyclin. *Circulation* 97: 99–107, 1998.
91. Nagababu E, Ramasamy S, and Rifkind JM. *S*-nitrosohemoglobin: a mechanism for its formation in conjunction with nitrite reduction by deoxyhemoglobin. *Nitric Oxide* 15: 20–29, 2006.
92. Napoli C, de Nigris F, Williams–Ignarro S, Pignalosa O, Sica V, and Ignarro LJ. Nitric oxide and atherosclerosis: An update. *Nitric Oxide* 15: 265–279, 2006.
93. Nase GP, Tuttle J, and Bohlen HG. Reduced perivascular PO_2 increases intirc oxide release from endothelial cells. *Am J Physiol Heart Circ Physiol* 285: H507–H515, 2003.
94. Olearczyk JJ, Ellsworth ML, Stephenson AH, Lonigro AJ, and Sprague RS. Nitric oxide inhibits ATP release from erythrocytes. *J Pharmacol Exp Ther* 309: 1079–1084, 2004.
95. Olearczyk JJ, Stephenson AH, Lonigro AJ, and Sprague RS. NO inhibits signal transduction pathway for ATP release from erythrocytes via its action on heterotrimeric G protein G_i. *Am J Physiol Heart Circ Physiol* 287: H748–754, 2004.
96. Pacher P and Szabo C. Role of peroxynitrite in the pathogenesis of cardiovascular complications of diabetes. *Curr Opin Pharmacol* 6: 136–141, 2006.
97. Palacios–Callender M, Hollis V, Frakich N, Mateo J, and Moncada S. Cytochrome *c* oxidase maintains mitochondrial respiration during partial inhibition by nitric oxide. *J Cell Sci* 120: 160–165, 2007.
98. Palm F, Buerk DG, Carlsson PO, Hansell P, and Liss P. Reduced nitric oxide concentration in the renal cortex of streptozotocin-induced diabetic rats: effects on renal oxygenation and microcirculation. *Diabetes* 54: 3282–3287, 2005.
99. Palmer LA, Gaston B, and Johns RA. Normoxic stabilization of hypoxia-inducible factor-1 expression and activity: redox-dependent effect of nitrogen oxides. *Mol Pharmacol* 58: 1197–1203, 2000.
100. Palmer RM, Ashton DS, and Moncada S. Vascular endothelial cells synthesize nitric oxide from L-arginine. *Nature* 333: 664–666, 1988.
101. Palmer RM, Ferrige AG, and Moncada S. Nitric oxide release accounts for the biological activity of endothelium-derived relaxing factor. *Nature* 327: 524–526, 1987.
102. Pardridge WM and Jefferson LS. Liver uptake of amino acids and carbohydrates during a single circulatory passage. *Am J Physiol* 228: 1155–1161, 1975.
103. Petersen LC. The effect of inhibitors on the oxygen kinetics of cytochrome *c* oxidase. *Biochim Biophys Acta* 460: 299–307, 1977.
104. Pryor WA, Houk KN, Foote CS, Fukuto JM, Ignarro LJ, Squadrito GL, and Davies KJ. Free radical biology and medicine: it's a gas, man! *Am J Physiol Regul Integr Comp Physiol* 291: R491–511, 2006.

105. Rayner BS, Wu BJ, Raftery M, Stocker R, and Witting PK. Human *S*-nitroso oxymyoglobin is a store of vasoactive nitric oxide. *J Biol Chem* 280: 9985–9993, 2005.
106. Rodríguez–Crespo I, Gerber NC, and Ortiz de Montellano PR. Endothelial nitric-oxide synthase. Expression in *Escherichia coli*, spectroscopic characterization, and role of tetrahydrobiopterin in dimer formation. *J Biol Chem* 271: 11462–11467, 1996.
107. Ruiz–Stewart I, Tiyyagura SR, Lin JE, Kazerounian S, Pitari GM, Schulz S, Martin E, Murad F, and Waldman SA. Guanylyl cyclase is an ATP sensor coupling nitric oxide signaling to cell metabolism. *Proc Natl Acad Sci USA* 101: 37–42, 2004.
108. Sandau KB, Fandrey J, and Brune B. Accumulation of HIF-1alpha under the influence of nitric oxide. *Blood* 97: 1009–1015, 2001.
109. Shaul PW. Endothelial nitric oxide synthase, caveolae and the development of atherosclerosis *J Physiol* 547: 21–33, 2003.
110. Shibata M, Ichioka S, and Kamiya A. Estimating oxygen consumption rates of arteriolar walls under physiological conditions in rat skeletal muscle. *Am J Physiol Heart Circ Physiol* 289: H295–300, 2005.
111. Shibata M, Ichioka S, and Kamiya A. Nitric oxide modulates oxygen consumption by arteriolar walls in rat skeletal muscle. *Am J Physiol Heart Circ Physiol* 289: H2673–2679, 2005.
112. Shibata M, Qin K, Ichioka S, and Kamiya A. Vascular wall energetics in arterioles during nitric oxide-dependent and -independent vasodilation. *J Appl Physiol* 100: 1793–1798, 2006.
113. Singel DJ and Stamler JS. Chemical physiology of blood flow regulation by red blood cells: the role of nitric oxide and *S*-nitrosohemoglobin. *Annu Rev Physiol* 67: 99–145, 2005.
114. Son H, Hawkins RD, Martin K, Kiebler M, Huang PL, Fishman MC, and Kandel ER. Long-term potentiation is reduced in mice that are doubly mutant in endothelial and neuronal nitric oxide synthase. *Cell* 87: 1015–1023, 1996.
115. Sprague RS, Ellsworth ML, Stephenson AH, and Lonigro AJ. Participation of cAMP in a signal-transduction pathway relating erythrocyte deformation to ATP release. *Am J Physiol Cell Physiol* 281: C1158–1164, 2001.
116. Stamler JS, Jia L, Eu JP, McMahon TJ, Demchenko IT, Bonaventura J, Gernert K, and Piantadosi CA. Blood flow regulation by *S*-nitrosohemoglobin in the physiological oxygen gradient. *Science* 276: 2034–2037, 1997.
117. Steppan J, Ryoo S, Schuleri KH, Gregg C, Hasan RK, White AR, Bugaj LJ, Khan M, Santhanam L, Nyhan D, Shoukas AA, Hare JM, and Berkowitz DE. Arginase modulates myocardial contractility by a nitric oxide synthase 1-dependent mechanism. *Proc Natl Acad Sci USA* 103: 4759–4764, 2006.
118. Stepuro TL and Zinchuk VV. Nitric oxide effect on the hemoglobin-oxygen affinity. *J Physiol Pharmacol* 57: 29–38, 2006.
119. Stuehr DJ. Mammalian nitric oxide synthases. *Biochim Biophys Acta* 1411: 217–230, 1999.
120. Stuehr DJ, Kwon NS, Nathan CF, Griffith OW, Feldman PL, and Wiseman J. *N* omega-hydroxy-L-arginine is an intermediate in the biosynthesis of nitric oxide from L-arginine. *J Biol Chem* 266: 6259–6263, 1991.
121. Suzuki T, Suematsu M, and Makino R. Organic phosphates as a new class of soluble guanylate cyclase inhibitors. *FEBS Lett* 507: 49–53, 2001.
122. Taylor PD and Poston L. The effect of hyperglycaemia on function of rat isolated mesenteric resistance artery. *Br J Pharmacol* 113: 801–808, 1994.
123. Thom SR, Bhopale V, Fisher D, Manevich Y, Huang PL, and Buerk DG. Stimulation of nitric oxide synthase in cerebral cortex due to elevated partial pressures of oxygen: an oxidative stress response. *J Neurobiol* 51: 85–100, 2002.
124. Thom SR, Bhopale VM, Velazquez OC, Goldstein LJ, Thom LH, and Buerk DG. Stem cell mobilization by hyperbaric oxygen. *Am J Physiol Heart Circ Physiol* 290: H1378–1386, 2006.
125. Thom SR and Buerk DG. Nitric oxide synthesis in brain is stimulated by oxygen. *Adv Exp Med Biol* 510: 133–137, 2003.
126. Thom SR, Fisher D, Zhang J, Bhopale VM, Cameron B, and Buerk DG. Neuronal nitric oxide synthase and *N*-methyl-D-aspartate neurons in experimental carbon monoxide poisoning. *Toxicol Appl Pharmacol* 194: 280–295, 2004.
127. Thom SR, Fisher D, Zhang J, Bhopale VM, Ohnishi ST, Kotake Y, Ohnishi T, and Buerk DG. Stimulation of perivascular nitric oxide synthesis by oxygen. *Am J Physiol Heart Circ Physiol* 284: H1230–1239, 2003.
128. Thomas DD, Liu X, Kantrow SP, and Lancaster JR, Jr. The biological lifetime of nitric oxide: implications for the perivascular dynamics of NO and O_2. *Proc Natl Acad Sci USA* 98: 355–360, 2001.
129. Tsai AG, Acero C, Nance PR, Cabrales P, Frangos JA, Buerk DG, and Intaglietta M. Elevated plasma viscosity in extreme hemodilution increases perivascular nitric oxide concentration and microvascular perfusion. *Am J Physiol Heart Circ Physiol* 288: H1730–1739, 2005.
130. Tsikas D, Boger RH, Sandmann J, Bode–Boger SM, and Frolich JC. Endogenous nitric oxide synthase inhibitors are responsible for the L-arginine paradox. *FEBS Lett* 478: 1–3, 2000.
131. Tsurumi Y, Murohara T, Krasinski K, Chen D, Witzenbichler B, Kearney M, Couffinhal T, and Isner JM. Reciprocal relation between VEGF and NO in the regulation of endothelial integrity. *Nat Med* 3: 879–886, 1997.
132. Tsutsui M, Shimokawa H, Morishita T, Nakashima Y, and Yanagihara N. Development of genetically engineered mice lacking all three nitric oxide synthases. *J Pharmacol Sci* 102: 147–154, 2006.
133. Valko M, Leibfritz D, Moncol J, Cronin MT, Mazur M, and Telser J. Free radicals and antioxidants in normal physiological functions and human disease. *Int J Biochem Cell Biol* 39: 44–84, 2007.
134. Vaughn MW, Huang KT, Kuo L, and Liao JC. Erythrocytes possess an intrinsic barrier to nitric oxide consumption. *J Biol Chem* 275: 2342–2348, 2000.
135. Vaughn MW, Kuo L, and Liao JC. Effective diffusion distance of nitric oxide in the microcirculation. *Am J Physiol* 274: H1705–H1714, 1998.
136. Vaughn MW, Kuo L, and Liao JC. Estimation of nitric oxide production and reaction rates in tissue by use of a mathematical model. *Am J Physiol* 274: H2163–2176, 1998.
137. Vukosavljevic N, Jaron D, Barbee KA, and Buerk DG. Quantifying the L-arginine paradox in vivo. *Microvasc Res* 71: 48–54, 2006.
138. Watford M. The urea cycle: a two-compartment system. *Essays Biochem* 26: 49–58, 1991.
139. Wei XQ, Charles IG, Smith A, Ure J, Feng GJ, Huang FP, Xu D, Muller W, Moncada S, and Liew FY. Altered immune responses in mice lacking inducible nitric oxide synthase. *Nature* 375: 408–411, 1995.
140. Yang J, Clark JW, Bryan RM, and Robertson CS. Mathematical modeling of the nitric oxide/cGMP pathway in the vascular smooth muscle cell. *Am J Physiol Heart Circ Physiol* 289: H886–897, 2005.
141. Yu J, deMuinck ED, Zhuang Z, Drinane M, Kauser K, Rubanyi GM, Qian HS, Murata T, Escalante B, and Sessa WC. Endothelial nitric oxide synthase is critical for ischemic remodeling, mural cell recruitment, and blood flow reserve. *Proc Natl Acad Sci USA* 102: 10999–11004, 2005.
142. Zani BG, and Bohlen HG. Transport of extracellular L-arginine via cationic amino acid transporter is required during in vivo endothelial nitric oxide production. *Am J Physiol Heart Circ Physiol* 289: H1381–1390, 2005.
143. Zheng JS, Yang XQ, Lookingland KJ, Fink GD, Hesslinger C, Kapatos G, Kovesdi I, and Chen AF. Gene transfer of human guanosine 5′-triphosphate cyclohydrolase I restores vascular tetrahydrobiopterin level and endothelial function in low renin hypertension. *Circulation* 108: 1238–1245, 2003.
144. Ziche M, Morbidelli L, Choudhuri R, Zhang HT, Donnini S, Granger HJ, and Bicknell R. Nitric oxide synthase lies downstream from vascular endothelial growth factor-induced but not basic fibroblast growth factor-induced angiogenesis. *J Clin Invest* 99: 2625–2634, 1997.

145. Zimmermann N and Rothenberg ME. The arginine-arginase balance in asthma and lung inflammation. *Eur J Pharmacol* 533: 253–262, 2006.
146. Zinchuk V and Borisiuk M. The effect of NO synthase inhibition on blood oxygen-carrying function during hyperthermia in rats. *Respir Physiol* 113: 39–45, 1998.
147. Zinchuk VV and Dorokhina LV. Blood oxygen transport in rats under hypothermia combined with modification of the L-arginine-NO pathway. *Nitric Oxide* 6: 29–34, 2002.
148. Zoccali C. Asymmetric dimethylarginine (ADMA): a cardiovascular and renal risk factor on the move. *J Hypertens* 24: 611–619, 2006.
149. Zweier JL, Samouilov A, and Kuppusamy P. Non-enzymatic nitric oxide synthesis in biological systems. *Biochim Biophys Acta* 1411: 250–262, 1999.

Address reprint requests to:
Donald G. Buerk
Departments of Physiology and Bioengineering
B400 Richards Building
3800 Hamilton Walk
University of Pennsylvania
Philadelphia, PA 19104

E-mail: buerk@seas.upenn.edu

Date of first submission to ARS Central, December 26, 2006; date of acceptance, January 13, 2007.

This article has been cited by:

1. Ashley M. Fuller, Charles Giardina, Lawrence E. Hightower, George A. Perdrizet, Cassandra A. Tierney. 2012. Hyperbaric oxygen preconditioning protects skin from UV-A damage. *Cell Stress and Chaperones* . [CrossRef]
2. Xuewen Chen, Donald G. Buerk, Kenneth A. Barbee, Patrick Kirby, Dov Jaron. 2011. 3D network model of NO transport in tissue. *Medical & Biological Engineering & Computing* **49**:6, 633-647. [CrossRef]
3. Mayumi Kajimura , Ryo Fukuda , Ryon M. Bateman , Takehiro Yamamoto , Makoto Suematsu . 2010. Interactions of Multiple Gas-Transducing Systems: Hallmarks and Uncertainties of CO, NO, and H2S Gas Biology. *Antioxidants & Redox Signaling* **13**:2, 157-192. [Abstract] [Full Text HTML] [Full Text PDF] [Full Text PDF with Links]
4. Kejing Chen, Roland N. Pittman, Aleksander S. Popel. 2009. Hemorrhagic shock and nitric oxide release from erythrocytic nitric oxide synthase: A quantitative analysis. *Microvascular Research* **78**:1, 107-118. [CrossRef]
5. Kejing Chen , Roland N. Pittman , Aleksander S. Popel . 2008. Nitric Oxide in the Vasculature: Where Does It Come From and Where Does It Go? A Quantitative Perspective. *Antioxidants & Redox Signaling* **10**:7, 1185-1198. [Abstract] [Full Text HTML] [Full Text PDF] [Full Text PDF with Links]
6. Douglas D. Thomas, Lisa A. Ridnour, Jeffrey S. Isenberg, Wilmarie Flores-Santana, Christopher H. Switzer, Sonia Donzelli, Perwez Hussain, Cecilia Vecoli, Nazareno Paolocci, Stefan Ambs, Carol A. Colton, Curtis C. Harris, David D. Roberts, David A. Wink. 2008. The chemical biology of nitric oxide: Implications in cellular signaling. *Free Radical Biology and Medicine* **45**:1, 18-31. [CrossRef]
7. Chris E. Cooper, Maria G. Mason, Peter Nicholls. 2008. A dynamic model of nitric oxide inhibition of mitochondrial cytochrome c oxidase. *Biochimica et Biophysica Acta (BBA) - Bioenergetics* **1777**:7-8, 867-876. [CrossRef]